Inorg. Chem. **2005**, *44*, 8539–8551

Tetrakis(thiadiazole)porphyrazines. 4. Direct Template Synthesis, Structure, General Physicochemical Behavior, and Redox Properties of Al^{III}, Ga^{III}, and In^{III} Complexes

Maria Pia Donzello,[†] Rita Agostinetto,[†] Svetlana S. Ivanova,[‡] Masato Fujimori,[§] Yosuke Suzuki,[§] Hirofumi Yoshikawa,[§] Jing Shen,[||] Kunio Awaga,*[,§] Claudio Ercolani,*[,†] Karl M. Kadish,*[,||] and Pavel A. Stuzhin[‡]

Dipartimento di Chimica, Università degli Studi di Roma "La Sapienza", P.le A. Moro 5, Roma, I-00185, Italy, Department of Organic Chemistry, Ivanovo State University of Chemical Technology, Friedrich Engels Pr-t 7, Ivanovo RF-153460, Russia, Department of Chemistry, Graduate School of Science, Furo-cho, Chikusa-ku, Nagoya 464-8602, Japan, and Department of Chemistry, University of Houston, Houston, Texas 77204-5003

Received May 30, 2005

Monometallic derivatives of tetrakis(1,2,5-thiadiazole)porphyrazine, [TTDPzH_2], with main group tervalent metal ions having the formulae [TTDPzMX] (TTDPz = tetrakis(1,2,5-thiadiazole)porphyrazinato dianion; M = Al^{III}, X = Cl^-, Br^-, OH^-; M = Ga^{III}, X = Cl^-, OH^-; M = In^{III}, X = AcO^-) were prepared and investigated by single-crystal X-ray analysis and IR and UV–vis spectroscopy as well as cyclic voltammetry and spectroelectrochemistry. The complexes [TTDPzMX] (M = Al^{III}, X = Cl^-, Br^-; M = Ga^{III}, X = Cl^-) were obtained by direct autocyclotetramerization of the precursor 3,4-dicyano-1,2,5-thiadiazole in hot quinoline in the presence of MX_3 salts (M = Al^{III}, Ga^{III}; X = Cl^-, Br^-) and were hydrolized to form the corresponding hydroxide derivatives, [TTDPzMOH]. The In^{III} complex, [TTDPzIn(OAc)], was obtained from the free-base macrocycle [TTDPzH_2] with $In(OH)(OAc)_2$ in CH_3COOH. A single-crystal X-ray study was made at 173 K on the two isostructural species [TTDPzMCl] (M = Al^{III}, Ga^{III}), which have space group $P\bar{1}$, with a = 12.470(14), b = 12.464(13), and c = 13.947(12) Å, α = 70.72(3), β = 79.76(3), and γ = 90.06(3)°, V = 2009.3(3) Å^3, and Z = 4 for [TTDPzAlCl] and a = 12.429(3), b = 12.430(3), and c = 13.851(3) Å, α = 70.663(6), β = 79.788(8), and γ = 89.991(9)°, V = 1983.3(7) Å^3, and Z = 4 for [TTDPzGaCl]. Square pyramidal coordination exists about the M^{III} centers, with Cl^- occupying the apical position (Al–Cl = 2.171(5) and Ga–Cl = 2.193(1) Å). Al^{III} and Ga^{III} are located at distances of 0.416(6) and 0.444(2) Å from the center of the N_4 system. The molecular packing consists of stacked double layers with internal and external average interlayer distances of 3.2 and 3.3 Å, respectively. IR spectra show ν(Al–Cl) at 345 cm^{-1} for [TTDPzAlCl], ν(Al–Br) at 330 cm^{-1} for [TTDPzAlBr], and ν(Ga–Cl) at 382 cm^{-1} for [TTDPzGaCl]. The UV–vis spectra in weakly basic (pyridine, DMF, DMSO) and acidic solvents (CF_3COOH, H_2SO_4) show the typical intense $\pi \rightarrow \pi^*$ transition bands in the Soret (300–400 nm) and Q-band regions (640–660 nm), the bands evidencing some dependence on the nature of the solvent, particularly in acidic solutions. Cyclic voltammetry, differential pulse voltammetry, and thin-layer spectroelectrochemical measurements in pyridine and dimethylformamide of the species [TTDPzMX] indicate reversible first and second one-electron reductions, whereas additional ill-defined reductions are observed at more negative potentials. The examined species are much easier to reduce than their phthalocyanine or porphyrin analogues as a result of the remarkable electron-attracting properties of the TTDPz macrocycle which contains annulated strongly electron-deficient thiadiazole rings.

Introduction

Substitution of external benzene rings in the phthalocyanine macrocycle [PcM] (Pc = phthalocyaninato dianion, Chart 1) by different heterocyclic moieties is a versatile method widely used to modify its spectral, coordination, and acid−base properties.[1] In recent years, our laboratories have synthesized and characterized new phthalocyanine-like macrocycles bearing different heterocyclic electron-deficient

* To whom correspondence should be addressed. E-mail: Claudio.ercolani@uniroma1.it (C.E.).
[†] Università degli Studi di Roma "La Sapienza".
[‡] Ivanovo State University of Chemical Technology.
[§] Graduate School of Science.
[||] University of Houston.

(1) Stuzhin, P. A.; Ercolani, C. In *The Porphyrin Handbook*; Kadish, K. M., Smith, K. M., Guilard, R., Ed.; Academic Press: Amsterdam, 2003; Vol. 15, Chapter 101, p 263.

10.1021/ic050866b CCC: $30.25
Published on Web 10/07/2005

Chart 1

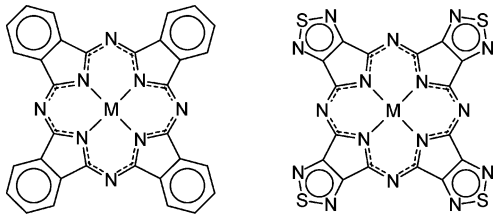

[PcM] [TTDPzM]

rings annulated to the pyrrole rings of the central porphyrazine core (1,2,5-thiadiazole,[2] 1,2,5-selenodiazole,[3] 1,4-diazepine,[4] and pyrazine rings[5]). Among these novel classes of macrocycles are the tetrakis(thiadiazole)porphyrazines, abbreviated as [TTDPzM] (Chart 1),[2,6] and the analogous Se-containing macrocycles, [TSeDPzM],[3] M being a divalent transition or nontransition metal ion.

Low-symmetry porphyrazine-type macrocycles formed by co-cyclotetramerization of a phthalocyanine precursor and a thia- or selenodiazole dicyano precursor were also prepared; their molecular and electronic structures were examined, and the UV−vis linear and nonlinear optical behavior was also examined in detail.[7]

A recent single-crystal X-ray study conducted on a series of [TTDPzM] species (M = $2H^1$, Fe^{II}, Co^{II}, Ni^{II}, Cu^{II}, Zn^{II}) showed the compounds to possess structural features which closely resemble those of their phthalocyanine analogues at a molecular level.[8] In this regard, it should be noted that this novel class of macrocycles and the parallel series of Se macrocycles, [TSeDPzM], are probably, from a structural and electronic point of view, the molecular systems which most closely approach the phthalocyanine macrocycle due to the similarity of their skeletal framework. Furthermore, π-conjugation, which permeates the entire macrocyclic unit, involves an equal number of π-electrons. The X-ray work, on the other hand, has evidenced new and remarkably different types of intermolecular contacts.[8] These are, in many cases, far from producing the type of columnar stacking found for phthalocyanines in their α and β forms, with quite different individual solid state arrays seen upon going from one metal derivative to another. The diversified solid-state arrangements of the molecular units in the different species is mainly due to the presence of the external heterocyclic rings carrying S and N atoms, which are able to generate a variety of new interunit contacts, including metal−nitrogen interactions in different α, β, and γ solid-state forms. This is a highly promising aspect of these compounds which might be used for the development of new types of solid-state materials, especially if account is taken that the species can be sublimed and thin solid films can be prepared and investigated for application purposes. New perspectives may also arise from solution studies of these species in view of their possible use as optical materials in the field of nonlinear optics or as new optical recording materials.

We have now extended our work on the "thiadiazoloporphyrazines" by the synthesis and characterization of novel complexes which incorporate main group tervalent metal ions, i.e., Al^{III}, Ga^{III}, and In^{III}. The physicochemical properties of this new class of macrocycles were investigated by single-crystal X-ray work and IR and UV−vis spectroscopy as well as cyclic voltammetry, differential pulse voltammetry, and spectroelectrochemistry. A detailed analysis of the available data is given in this paper and provides information on the molecular and electronic structure and the redox properties of these new species. The X-ray work carried out on the aluminum chloride and gallium chloride species, [TTDPzAlCl] and [TTDPzGaCl], further indicates that the presence of heterocyclic rings externally annulated to the porphyrazine core and bearing S and N atoms strongly influences the solid-state arrangement. The electrochemical measurements carried out on [TTDPzMX] point to the remarkable electron-deficient properties of the porphyrazine macrocycle and allow interesting comparisons with the related class of phthalocyanine analogues and other porphyrazine systems recently studied by our groups.[2−7]

Results and Discussion

Synthesis. The common synthetic procedure previously used for the preparation of the metal complexes [TTDPzM] (M = Mn^{II} to Zn^{II}) first involved the synthesis of the Mg^{II} derivative, [TTDPzMg(H_2O)], by the template condensation of 3,4-dicyano-1,2,5-thiadiazole (DCTD) with magnesium propylate in propanol, followed by its demetalation to the free-base macrocycle [$TTDPzH_2$] and then incorporation of the desired metal ion by reaction with the appropriate metal salt in DMSO.[2] This three-step procedure was needed since the precursor DCTD, unlike phthalodinitrile, the phthalocyanine precursor, failed to react directly with the divalent transition metal salts to give reasonable yields of the metalated macrocyclic complexes. A direct cyclotetramerization, implying metal complexation, is instead possible for the main group tervalent metal ions. Thus, DCTD reacts with anhydrous Al^{III} and Ga^{III} halides, the best results being achieved by carrying out the reaction in hot quinoline. In the case of the In^{III} salts (halide or acetate) a direct

(2) (a) Stuzhin, P. A.; Bauer, E. M.; Ercolani, C. *Inorg. Chem.* **1998**, *37*, 1533. (b) Bauer, E. M.; Cardarilli, D.; Ercolani, C.; Stuzhin, P. A.; Russo, U. *Inorg. Chem.* **1999**, *38*, 6114.
(3) (a) Bauer, E. M.; Ercolani, C.; Galli, P.; Popkova, I. A.; Stuzhin, P. A. *J. Porphyrins Phthalocyanines* **1999**, *3*, 371. (b) Angeloni, S.; Bauer, E. M.; Ercolani, C.; Popkova, I. A.; Stuzhin, P. A. *J. Porphyrins Phthalocyanines* **2001**, *5*, 881.
(4) (a) Donzello, M. P.; Ercolani, C.; Stuzhin, P. A.; Chiesi-Villa, A.; Rizzoli, C. *Eur. J. Inorg. Chem.* **1999**, 2075. (b) Donzello, M. P.; Dini, D.; D'Arcangelo, G.; Ercolani, C.; Zhan, R.; Ou, Z.; Stuzhin, P. A.; Kadish, K. M. *J. Am. Chem. Soc.* **2003**, *125*, 14190.
(5) (a) Donzello, M. P.; Ou, Z.; Monacelli, F.; Ricciardi, G.; Rizzoli, C.; Ercolani, C.; Kadish, K. M. *Inorg. Chem.* **2004**, *43*, 8626. (b) Donzello, M. P.; Ou, Z.; Dini, D.; Meneghetti, M.; Ercolani, C.; Kadish, K. M. *Inorg. Chem.* **2004**, *43*, 8637.
(6) Stuzhin, P. A.; Pozdysheva, E. A.; Mal′chugina, O. V.; Popkova, I. A.; Ercolani, C. Tetrakis(thiadiazole)porphyrazines. 3. Study of acid−base properties and stability of tetrakis-3,4-(1,2,5-thiadiazole)porphyrazine in sulfuric acid solutions. *Khim. Geterotsikl. Soed.* **2005**, 278 [*Chem. Heterocycl. Compd.* **2004**, 278 (English translation)].
(7) (a) Kudrik, E. V.; Bauer, E. M.; Ercolani, C.; Stuzhin, P. A.; Chiesi-Villa, A.; Rizzoli, C. *Mendeleev Commun.* **2001**, 45. (b) Donzello, M. P.; Ercolani, C.; Gaberkorn, A.; Kudrik, E. V.; Meneghetti, M.; Marcolongo, G.; Rizzoli, C.; Stuzhin, P. A. *Chem.*—Eur. J. **2003**, *9*, 4009.
(8) (a) Fujimori, M.; Suzuki, Y.; Yoshikawa, H.; Awaga, K. *Angew. Chem., Int. Ed.* **2003**, *42*, 5863. (b) Suzuki, Y.; Fujimori, M.; Yoshikawa, H.; Awaga, K. *Chem.*—Eur. J. **2004**, *10*, 5158.

Scheme 1

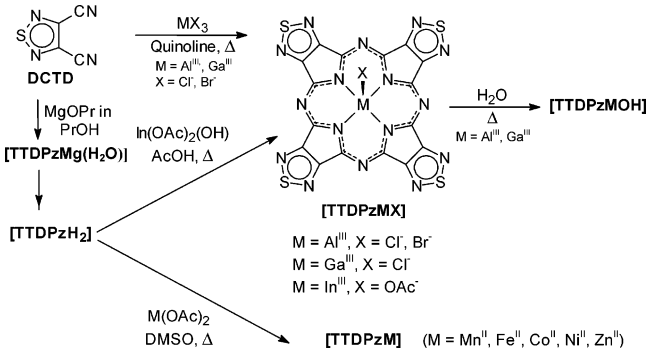

macrocyclization also takes place, but the above-mentioned three-step procedure[2] is preferred since it affords higher yields of [TTDPzIn(OAc)] and requires a less time-consuming purification procedure.

Elemental and thermogravimetric analysis (see Experimental Section) combined with IR spectra indicate that all of the species were obtained in their solvated forms (H_2O and quinoline; hereafter omitted unless strictly required). The amount of H_2O and quinoline (if present) was found to vary slightly from preparation to preparation for the different species. Scheme 1 summarizes the procedures followed for the synthesis of the tetrakis(thiadiazole)porphyrazines prepared previously[2] and those described in this article.

The metal−halogen bond in halides of compounds with group XIII metals is known to be unstable to hydrolysis. Since the first synthesis of the phthalocyanine species [PcAlCl],[9] hydrolysis of the Al−Cl bond was studied under a variety of conditions and generally leads to formation of the corresponding hydroxo species [PcAlOH].[9−12] Similar reactions were also observed for the formation of [(P)AlOH] compounds (P = porphyrin dianion) from the corresponding chlorides.[13−17]

The M−Cl bonds in [TTDPzAlCl] and [TTDPzGaCl] undergo slow hydrolysis in air. They can be easily hydrolyzed in a water suspension to give the corresponding hydroxo complexes [TTDPzAlOH] and [TTDPzGaOH]. The In^{III} acetate complex does not hydrolyze under similar conditions and any attempt to accomplish this in the presence of hydroxide leads to reduction of the macrocycle. The observed facile hydrolysis of the Al−Cl and Ga−Cl bonds in the respective [TTDPzAlCl] and [TTDPzGaCl] complexes, as compared to what is observed for related porphyrin and phthalocyanine analogues, is evidently due to the electron-attracting effect of the peripheral 1,2,5-thiadiazole rings, which increases the ionic character of the M−Cl bond, this in turn promoting exchange of Cl^- with the nucleophilic OH^-.

Table 1. Crystallographic Data for [TTDPzAlCl] and [TTDPzGaCl]

param	[TTDPzAlCl]	[TTDPzGaCl]
formula	$C_{16}AlClN_{16}S_4$	$C_{16}ClGaN_{16}S_4$
fw	606.99	649.73
cryst system	triclinic	triclinic
space group	$P\bar{1}$ (No. 2)	$P\bar{1}$ (No. 2)
a/Å	12.470(14)	12.429(3)
b/Å	12.464(13)	12.430(3)
c/Å	13.947(12)	13.851(3)
α/deg	70.72(3)	70.663(6)
β/deg	79.76(3)	79.788(8)
γ/deg	90.06(3)	89.991(9)
V/Å^3	2009.3(3)	1983.3(7)
Z	4	4
μ(Mo Kα)/mm^{-1}	0.703	1.997
unique reflns	5126 ($2\theta < 45°$)	8707 ($2\theta < 55°$)
$R(F)$ ($F > 4\sigma$)	0.1626	0.0489

X-ray Work on the Complexes [TTDPzMCl] (M = Al^{III}, Ga^{III}). Single crystals of [TTDPzAlCl] and [TTDPzGaCl] were grown by vacuum sublimation at 420 and 500 °C, respectively, under a continuous N_2 flow of 50 mL/min. The level of their crystallinity was not, however, very high. The poor crystallinity observed, verified also for their phthalocyanine analogues,[18,19] is presumably caused by the relative sliding of adjacent double layers (see discussion below), making the crystals mosaic. It is worth noting that attempts to prepare single crystals without the gas flow were unsuccessful. The structures were elucidated by single-crystal X-ray analysis, and Table 1 summarizes the crystallographic data.

The two complexes are isostructural, consisting of a stacking of double-layered structures. Figure 1 depicts top and side views of the structure for the GaCl complex. Both complexes show similarities with the corresponding phthalocyanine species, [PcAlCl] and [PcGaCl],[18,19] especially intramolecularly. However, differences are shown at the level of the intermolecular contacts, which influence the cell construction and the overall structure. This appears to be related to the presence of the S and N atoms in the thiadiazole rings of the porphyrazine macrocycle, as was the case for the previously reported [TTDPzM] complexes.[8] For the currently examined Al^{III} and Ga^{III} species, [TTDPzMCl], similar to the findings for the phthalocyanine analogues,[18,19] the metal centers exhibit a square pyramidal structure. Selected averaged bond distances are summarized in Table 2 together with those of related species.

Al^{III} and Ga^{III} in the two TTDPz complexes are displaced out of the plane of the inner N_4 chromophore toward the axial Cl^- (Al−Cl = 2.171(5) and Ga−Cl = 2.193(1) Å) with average distances from the center of the N_4 system (C_t) of 0.416(6) Å for Al^{III} and 0.444(2) Å for Ga^{III}. These M−C_t distances are only slightly longer than those found for their

(9) Barrett, P. A.; Dent, C. E.; Linstead, R. P. *J. Chem. Soc.* **1936**, 1719.
(10) Owen, J. E.; Kenney, M. E. *Inorg. Chem.* **1962**, *1*, 334.
(11) Chen, Y.; Subramanian, L. R.; Fujitsuka, M.; Ito, O.; O'Flaherty, S.; Blau, W. J.; Schneider, T.; Dini, D.; Hanack, M. *Chem.*—Eur. J. **2002**, *8*, 4248.
(12) Shaposhnikov, G. P.; Borodkin, V. F.; Fedorov, M. I. *Izv. Vyssh. Uchebn. Zaved., Khim. Khim. Tekhnol.* **1981**, *24*, 1485; *Chem Abstr.* **1982**, *97*, 30632.
(13) Kaizu, Y.; Misu, N.; Tsuji, K.; Kaneko, Y.; Kobayashi, H. *Bull. Chem. Soc. Jpn.* **1985**, *58*, 103.
(14) Parzuchowski, P. G.; Kampf, J. W.; Rozniecka, E.; Kondratenko, Y.; Malinowska, E.; Meyerhoff, M. E. *Inorg. Chim. Acta* **2003**, *355*, 302.
(15) Kadish, K. M.; Cornillon, J. L.; Coutsolelos, A.; Guilard, R. *Inorg. Chem.* **1987**, *26*, 4167.
(16) Cocolios, P.; Guilard, R.; Bayeul, D.; Lecomte, C. *Inorg. Chem.* **1985**, *24*, 2058.
(17) Inhoffen, H. H.; Buchler, J. W. *Tetrahedron Lett.* **1968**, 2057.
(18) Wynne, K. J. *Inorg. Chem.* **1984**, *23*, 4658.
(19) Yamasaki, K.; Okada, O.; Inami, K.; Oka, K.; Kotani, M.; Yamada, H. *J. Phys. Chem. B* **1997**, *101*, 13.

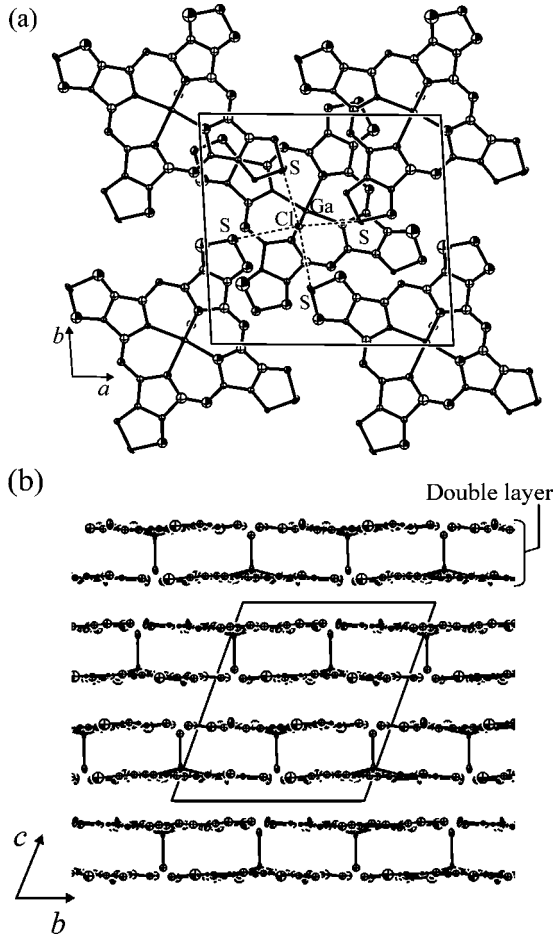

Figure 1. Top (a) and side (b) views of the double-layered structure in [TTDPzGaCl].

Table 2. Selected Average M−Cl, M−N, M−C_t, and N−C_t Bond Distances (Å) in the Al^{III} and Ga^{III} Complexes of Tetrapyrrolic Macrocycles

complex	M−Cl	M−N	M−C_t	N−C_t
[TTDPzAlCl]	2.171(5)	2.006(11)	0.416(6)	1.96(2)
[PcAlCl][a]	2.179(6)	1.98(3)	0.410(6)	1.94
[TTDPzGaCl]	2.193(1)	2.012(4)	0.444(2)	1.962(5)
[PcGaCl][a]	2.217(1)	1.983(4)	0.439(1)	1.93
[OEPGaCl][b]	2.240	2.035(4)	0.398(18)	2.00
[TPPGaCl][c]	2.176	2.022	0.318	2.00

[a] Data from ref 18. [b] Data from ref 20. [c] Data from ref 21.

Pc analogues (Table 2).[18,19] The longer M−C_t distance for Ga^{III} as compared to that of Al^{III} is in keeping with the higher ionic radius of Ga^{III}. By extension of the comparison with the data for the Pc complexes (Table 2), the present porphyrazine species show longer M−N bond distances, particularly in the case of the Ga species, and shorter apical M−Cl distances, both macrocycles showing little distortion from planarity. Structural data for two porphyrin GaCl species, i.e., [OEPGaCl][20] and [TPPGaCl][21] (OEP = octaethylporphyrin, TPP = tetraphenylporphyrin), are also shown in Table 2. As can be seen, the porphyrin macrocycle, which has a central cavity larger than that of phthalocyanine and the currently described porphyrazine macrocycles, locates the metal center with a markedly shorter Ga−C_t distance, in line with expectation.

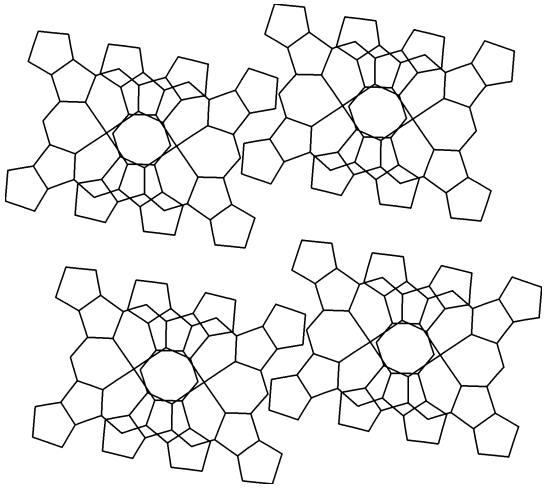

Figure 2. Concave−concave overlapping in [TTDPzGaCl].

The distance between the two least-squares planes in a double layer (Figure 1) is ca. 3.2 Å. As can be seen from the figure, in a double-layered section of the structure the Cl^- ion of the bottom macrocycle is approached by four porphyrazine units residing on the top layer with Cl···S contacts of ca. 3.4 Å. Moreover, in the present species, the porphyrazine units, unlike their phthalocyanine counterparts in the [PcMCl] analogues,[22] partly overlap (convex−convex overlapping) and, worthy of notice, some interunit interatomic distances involving heteroatoms of the thiadiazole rings (C_α···N_{het} and S···N_{meso}) are also present and reach values as short as 3.2−3.3 Å.

Stacking of the double layers also involves a consistent overlap between adjacent macrocyclic units belonging to different double layers (concave−concave overlap). Figure 2 shows that this overlap is characterized by a slipping along the $N_{meso}-N_{meso}$ axis and is such that a *meso*-N of one molecule is positioned just below and above the metal atoms of adjacent molecules.

The double layers are stacked along the *c* axis with only $\pi-\pi$ interactions at the short average distance of ca. 3.3 Å, but the shortest interatomic distances between overlapping adjacent molecules reach values of 3.1−3.2 Å. It may be postulated that these short intermolecular contacts, which are comparable with or below the values of the van der Waals distances (ca. 3.4 Å), might lead, by partial oxidation or reduction, to the formation of electrically conducting materials, as was the case for related phthalocyanine analogues[18] and other similar macrocyclic systems.[23] As a further comment, we note that the two isostructural complexes [TTDPzMCl] (M = Al^{III}, Ga^{III}), most likely as a result of the specific nature of the interunit contacts determined by the heteroatoms present in the porphyrazine macrocycle, show structural features different from those found for the phthalocyanine analogues.[22] For these latter species, in fact,

(20) Brancato-Buentello, K. E.; Coutsolelos, A. G.; Scheidt. W. R. *Acta Crystallogr*. **1996**, *C52*, 2707.
(21) Coutsolelos, A.; Guilard, R.; Bayeul, D.; Lecomte, C. *Polyhedron* **1986**, *5*, 1157.
(22) Engel, M. K. In *The Porphyrin Handbook*; Kadish, K. M., Smith, K. M., Guilard, R., Ed.; Academic Press: Amsterdam, 2003; Vol, 20, Chapter 122, p 54.

Table 3. M−X Stretching Vibrations for the [TTDPzMX] Complexes (X = Cl, Br) and Related Species

		ν(M−X), cm^{-1}			
M	X	[TTDPzMX]	[PcMX]	[PMX]	[Ph_8PzMX][a]
Al^{III}	Cl^-	345	440[b]		338
Ga^{III}	Cl^-	382	351[c]	332 (P = OEP)[d] 352 (P = TPP)[d]	345
Al^{III}	Br^-	330	397[b]		260

[a] From ref 25. [b] From ref 24. [c] From ref 11. [d] From ref 16.

the concave−concave double-layer arrangement seems to be rather regulated by the nature of the metal ions since the Al^{III} and Ga^{III} species in this case are slipped along different axes, i.e., $N_{meso}-N_{meso}$ and $N_{pyr}-N_{pyr}$, respectively.

IR Spectra. The IR spectra of the [TTDPzMX] complexes closely resemble those of the previously reported [TTDPzM] complexes.[2] Characteristic skeletal modes of the [TTDPz] macrocycle appear at 1550−1530 and 1520−1500 cm^{-1} ($C_\alpha{=}N_{meso}$), 1280−1260 cm^{-1} ($C_\beta{=}C_\beta$ coupled with $C_\beta{=}N$ of the annulated ring), 1130−1010 cm^{-1} ($C_\alpha{=}N_{pyr}$), and 740−730 and 695−665 cm^{-1} (out-of-plane deformations), and vibrations of the 1,2,5-thiadiazole ring produce absorptions at 830−810 and 770−750 cm^{-1} (N−S stretching), 895−865 and 625−610 cm^{-1} (annulated ring deformations), and 515−510 cm^{-1} (annulated ring torsion). The type of metal ion in the macrocycle has a more pronounced influence on the vibrations of the bonds close to the coordination center, like for instance the $C_\alpha{=}N_{pyr}$ vibration which is present in the 1130−1010 cm^{-1} region. Although this vibration appears as a single strong absorption for the Al^{III} complexes, [TTDPzAlX], as well as for the square planar complexes of the divalent metals, i.e., [TTDPzCu] and its analogues,[2b] a splitting of this band becomes evident for the Ga^{III} and In^{III} species. This splitting effect is caused by a lowering of the effective symmetry at the central core, resulting from an out-of-plane displacement of the metal ion and the associated doming of the macrocycle. The same type of splitting is observed for the band assigned to the out-of-plane vibrations of the macrocycle at 695−665 cm^{-1}.

Table 3 lists the measured M−Cl and M−Br stretching vibrations for the investigated Al^{III} and Ga^{III} species and some of their porphyrin,[16] phthalocyanine,[11,24] and porphyrazine[25] analogues. The vibrations and related assignments are important for a correct identification of the species studied. Support for the assignments of ν(Al−Cl) at 345 cm^{-1} and ν(Ga−Cl) at 382 cm^{-1} for [TTDPzAlCl] and [TTDPzGaCl], respectively, is given in the absence of other significant spectral modifications in all the region explored (4000−200 cm^{-1}), by the disappearance of these IR bands consequent to hydrolysis of the M−Cl bonds to give species with M−OH bonds (see Figure S1 in the Supporting Information for the Al−Cl species).

It should be noted that the ν(Al−X) values (X = Cl^-, Br^-) for the present Al^{III} species are seen at much lower frequencies than those observed for the phthalocyanine analogues[24] and approach values for the corresponding β-phenyl-substituted porphyrazine derivatives (Table 3).[25] This indicates much weaker Al−X bonds in the [TTDPzAlX] species and is in agreement with their higher hydrolizability as has been discussed above. The higher value of ν(Al−Cl) for [PcAlCl] (440 cm^{-1}, Table 3) with respect to that observed for [PcGaCl] (351 cm^{-1}) is as expected. However, for the present [TTDPz] complexes ν(Al−Cl) is at lower frequency (345 cm^{-1}) than ν(Ga−Cl) (382 cm^{-1}). The reason for this reversal of frequencies is unknown if account is taken of the close M−Cl bond distances observed for the Pc and TTDPz couples of complexes (Table 2).

The O−H stretching vibrations cannot be easily identified in the IR spectra of the hydroxo species [TTDPzMOH], very likely because of the involvement of the OH^- group in hydrogen bonding, either with the water molecules or by intermolecular contacts at the level of the thiadiazole rings.

Solution Studies. UV−Vis Spectra. The UV−vis spectra of the monometallic species [TTDPzMX] (M = Al^{III}, Ga^{III}, In^{III}) were recorded in both slightly basic solvents (pyridine, DMF, DMSO) and acidic solvents (CF_3COOH, H_2SO_4). Representative spectra for the chloride and hydroxide Al^{III} complexes are shown in Figure 3, and the spectral data are summarized in Table 4.

The spectra in basic solvents show in all cases the typical pattern commonly present in porphyrazine-type macrocycles; i.e., there is an intense Q band in the region 640−660 nm accompanied by vibronic satellites at higher energy and a broad comparatively less intense Soret band envelope in the region 300−400 nm. No dependence of the Q-band position is observed for the Al^{III} or Ga^{III} complexes by changing the type of solvent, and minimal spectral variations are seen for the same metal derivative upon changing the axial ligand, Cl^- (Br^-) or OH^- (see Figure 3A,B for [TTDPzAlX]; X = Cl^-, OH^-). A shift of the Q-band, although confined within a narrow range (13−15 nm), is instead seen in each selected solvent (pyridine, DMF, DMSO) as a function of the central metal ion, with the Q-band maximum systematically shifted toward longer wavelengths in the order $Ga^{III} < Al^{III} < In^{III}$. The position of the Q-band in pyridine, for instance, is 645 nm for [TTDPzGaCl], 647 nm for [TTDPzAlCl], and 658

(23) (a) Dirk, C. W.; Inabe, T.; Schoch, K. F.; Marks, T. J. *J. Am. Chem. Soc.* **1983**, *105*, 1719. (b) Diel, B. N.; Inabe, T.; Lyding, J. F.; Schoch, K. F.; Kannewurf, K. R.; Marks, T. J. *J. Am. Chem. Soc.* **1983**, *105*, 1551. (c) Inabe, T.; Gaudiello, J. G.; Moguel, M. K.; Lyding, J. F.; Burton, R. L.; McCarthy, W. J.; Kannewurf, K. R.; Marks, T. J. *J. Am. Chem. Soc.* **1986**, *108*, 7595. (d) Almeida, M.; Kanayzidis, M. G.; Tonge, L. M.; Marks, T. J.; Marcy, H. O.; McCarthy, W. J.; Kannewurf, K. R. *Solid State Commun.* **1987**, *63*, 457. (e) Yakushi, K.; Yamakado, H.; Ida, T.; Ugawa, A. *Solid State Commun.* **1991**, *78*, 919. (f) Hanack, M.; Lang, M. *Adv. Mater.* **1994**, *6*, 819. (g) Moubaraki, B. P.; Benlian, D.; Baldy, A.; Pierrot, A. *Acta Crystallogr.* **1989**, *C45*, 393. (h) Capobianchi, A.; Ercolani, C.; Paoletti, A. M.; Pennesi, G.; Rossi, G.; Chiesi-Villa, A.; Rizzoli, C. *Inorg. Chem.* **1993**, *32*, 4605. (i) Capobianchi, A.; Paoletti, A. M.; Pennesi, G.; Rossi, G.; Caminiti, R.; Ercolani, C. *Inorg. Chem.* **1994**, *33*, 4635. (j) Paoletti, A. M.; Pennesi, G.; Rossi, G.; Ercolani, C. *Inorg. Chem.* **1995**, *34*, 4780. (k) Capobianchi, A.; Pennesi, G.; Paoletti, A. M.; Rossi, G.; Caminiti, R.; Sadun, C.; Ercolani C. *Inorg. Chem.* **1996**, *35*, 4643. (l) Caminiti, R.; Donzello, M. P.; Ercolani, C.; Sadun, C. *Inorg. Chem.* **1998**, *37*, 4210.

(24) Linsky, J. P.; Paul, T. R.; Nohr, R. S.; Kenney, M. E. *Inorg. Chem.* **1980**, *19*, 3131.

(25) Ivanova, S. S.; Stuzhin, P. A. *Russ. J. Coord. Chem.* **2004**, *30*, 765 (English translation of : *Koord. Khim.* **2004**, *30*, 813).

Table 4. Qualitative UV−Vis Spectra of the [TTDPzMX] Complexes in Different Solvents

		abs bands, λ_{max}, nm						
		Soret region			Q-band region[a]			
complex	solvent							
[TTDPzAlCl]	Py	340	364 sh	393 sh	590	622		**647**
	DMF	333	355 sh	385 sh	586	617		**643**
	DMSO	340			590	623		**649**
	CF_3COOH	329			583	620	642 sh	**648**
	H_2SO_4	330			600 sh		649 sh	**660**
[TTDPzAlBr]	Py	340	364 sh	392 sh	586	620		**646**
	DMF	331	359 sh		586	618		**643**
	DMSO	343			592	627		**651**
	CF_3COOH	329			583	622 sh	643 sh	**647**
	H_2SO_4	330				602 sh	649 sh	**660**
[TTDPzAlOH]	Py	340	363 sh	392 sh	588	620		**648**
	DMF	326	351 sh		585	618		**643**
	DMSO	342			592	629 sh		**652**
	CF_3COOH	329			583	620 sh	643 sh	**647**
	H_2SO_4	330			602 sh		649 sh	**660**
[TTDPzGaCl]	Py	337	367 sh	400 sh	585	617		**645**
	DMF_b	323 sh			584	615		**641**
	DMSO[b]	338			587	624		**647**
	CF_3COOH	329			582	615	640 sh	**645**
	H_2SO_4	330			597 sh		648 sh	**659**
[TTDPzGaOH]	Py	342	370 sh	393 sh	587	618		**646**
	DMF	331			583	615		**640**
	DMSO	340			589	624		**647**
	CF_3COOH	329			582	616 sh	640 sh	**646**
	H_2SO_4	330			599 sh	612 sh	649 sh	**659**
[TTDPzIn(OAc)]	Py	321	365 sh	390 sh	602			**658**
	DMF[a]	369			598 sh			**654**
	DMSO	357 sh			609	636 sh		**658**
	CF_3COOH	328	371sh		594	629		**646**[c]
	H_2SO_4	317	390 sh		618 sh			**671**

[a] The most intense Q-band is given in bold type (see Figure 3 for selected spectra). [b] Spectra taken immediately after dissolution; spectral changes are observed as a function of time. [c] A shoulder is present at 652 nm.

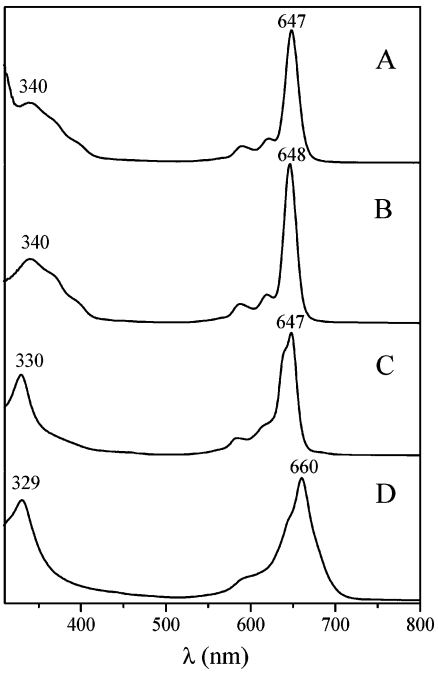

Figure 3. UV−vis spectra of [TTDPzAlCl] in pyridine (A) and [TTDPzAlOH] in pyridine (B), CF_3COOH (C), and 96% H_2SO_4 (D).

nm for [TTDPzIn(OAc)] (Table 4). The observed order might reflect a lowering of the HOMO due to higher stability of the central M−N σ-bonds in the Al^{III} and Ga^{III} complexes and to some destabilization of the LUMO for the Ga^{III} complex due to a contribution of the 3d orbitals which interact with the π*-MOs of the macrocycle. In the case of

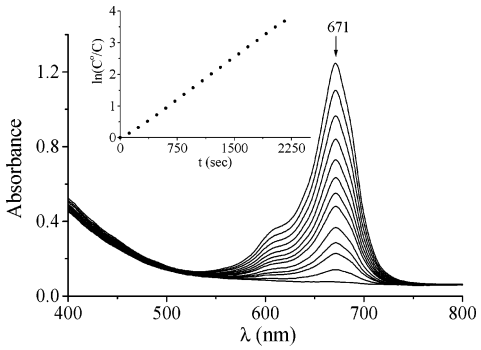

Figure 4. Spectral changes for [TTDPzIn(OAc)] in 16.9 M H_2SO_4 at 51 °C. Spectral curves are registered at 90 s intervals. The inset shows linear first-order dependence.

the In^{III} species, a stronger solvatochromic effect is observed in basic solvents due to the ability of the central metal ion to attain six-coordination in a cis-fashion, thus producing a more significant departure of the macrocycle from planarity.

The UV−vis spectra of [TTDPzMX] in acidic media compared to those seen in basic solvents provide some information as to the kind of interaction which occurs between the macrocycle and the acidic solvent. In the order from the basic solvent (pyridine) to a CF_3COOH solution of the Al−X and Ga−X complexes (X = Cl^-, OH^-) (see Figure 3C for [TTDPzAlOH]), the Q-band position remains unchanged (645−648 nm). This seems to suggest that an acid−base interaction, if occurring, is probably localized peripherally on the N atoms of the heterocyclic moieties. The additional shoulder on the blue side of the Q band in

Table 5. Kinetic Parameters of the Demetalation Process for the [TTDPzMX] Species in 16.9 M H_2SO_4

	k_{obs}, s^{-1}		
T, °C	[TTDPzAlOH]	[TTDPzGaOH]	[TTDPzIn(OAc)]
25	too slow	$(1.67 \pm 0.01) \times 10^{-6}$	$(1.98 \pm 0.01) \times 10^{-4}$
51	$(3.88 \pm 0.07) \times 10^{-5}$	$(1.87 \pm 0.10) \times 10^{-4}$	$(1.81 \pm 0.01) \times 10^{-3}$
65	$(1.71 \pm 0.04) \times 10^{-4}$	$(7.09 \pm 0.03) \times 10^{-4}$	$(5.55 \pm 0.04) \times 10^{-3}$
E_a, kJ/mol	95 ± 7	78 ± 4	69 ± 3

the spectra of the Al^{III} and Ga^{III} complexes in CF_3COOH gains in intensity and appears as the main peak for the In^{III} complex (647 nm).

As to the Soret band region, the complex envelope having a maximum at ca. 340 nm for the Al^{III} and Ga^{III} complexes is shifted hypsochromically by ca. 5−10 nm upon going from a basic solvent to CF_3COOH and appears as a sharp peak in the acidic medium due to the lack of shoulders at higher wavelengths (compare spectra A−C in Figure 3). Since these shoulders are due to n(N) → π^* transitions of the 1,2,5-thiadiazole rings, their disappearance in acidic media can be related to an acid−base interaction.

A broader Q-band envelope, shifted bathochromically to 659−670 nm, is seen for all of the [TTDPzMX] complexes (M = Al^{III}, Ga^{III}, In^{III}) in H_2SO_4 (see Figure 3D for M = Al^{III}). It is suggested here that the bathochromic shift observed in this solvent is caused by an interaction of the acid with the 1,2,5-thiadiazole rings in combination with a protonation of one of the *meso*-N atoms of the porphyrazine macrocycle.

Solutions of all [TTDPzMX] complexes in concentrated (90−98%) H_2SO_4 are less stable than in CF_3COOH, and upon sitting, they slowly discolor at room temperature, with more rapid changes observed at higher temperatures. Figure 4 shows the characteristic spectral changes occurring as a function of time for [TTDPzIn(OAc)] in 16.9 M (91%) H_2SO_4 at 51 °C. These spectral changes follow a strict first-order kinetic law, and the related constants (k_{obs}) were determined at different temperatures (see Table 5). Since under similar experimental conditions the unmetalated macrocycle [$TTDPzH_2$] undergoes very rapid decomposition (k_{obs}= $(9.11 \pm 1.02) \times 10^{-3}$ s^{-1} in 17.1−18.4 M H_2SO_4 at 25 °C [6]), the lower k_{obs} values obtained suggest that demetalation of [TTDPzMX] to give the free-base macrocycle is the rate-determining step followed by rapid decomposition of the metal-free compound. From Table 5 it is seen that the stability of the [TTDPzMX] complexes to demetalation increases in the order In^{III} < Ga^{III} < Al^{III}, which reflects the stability of the M−N bonds. The activation energy, E_a, also increases in this order, going from 69 ± 3 kJ/mol for In^{III} to 95 ± 7 kJ/mol for Al^{III}. Complexes with In^{III} have a lower stability to demetalation due to their weaker σ-binding ability which relates to the larger ionic radius and consequent larger out-of-plane displacement of the metal center from the porphyrazine plane.

Electrochemical Studies. The electrochemistry of [TTDPzMX] was investigated by cyclic voltammetry and thin-layer spectroelectrochemistry in pyridine. Some of the compounds were also examined by cyclic voltammetry and differential pulse voltammetry (DPV) in DMF for comparison with related [PcMX] derivatives under the same solution conditions.

Four one-electron reductions were expected for the currently investigated TTDPz derivatives, in line with the findings for related compounds containing Ph_8DzPz[4b] or $Py_8TPyzPz$[5b] macrocycles, but these were not easily observed since the voltammetric data are "complicated" by the presence of equilibria involving solvent and anion binding to the neutral species and different solvated or possibly aggregated forms of the electroreduced species. The measured potentials were found to depend on both chemical (compound specific) and electrochemical factors. The compound specific factors are the type of central metal ion (Al^{III}, Ga^{III}, or In^{III}), the solvent (pyridine or DMF), and the anionic axial ligand (Cl^-, OH^-, OAc^-, or ClO_4^-) while the electrochemical factors involve experimental parameters associated with the measurement process itself, five examples being (i) the potential scan rate, (ii) the potential scan range, (iii) the number of potential scans (single or multiple scans), (iv) the type of measurement technique, i.e., regular CV, thin-layer CV, or DPV, and (v) the concentration of the electroactive species. A change in any of the above conditions was seen to result in different current−voltage curves due to changes in the position of equilibria involving the species being electroreduced in each step.

In the potential window explored for pyridine or DMF (+0.7 to −2.0 V vs SCE) only cathodic (reduction) processes were observed for all of the examined [TTDPzMX] complexes. The measured half-wave potentials ($E_{1/2}$, V vs SCE) are summarized in Table 6 together with data for several related phthalocyanines[26−28] and porphyrin analogues.[29−31]

It is known that the Al^{III}, Ga^{III}, and In^{III} ions are redox inactive in phthalocyanine[28,32] and porphyrin complexes[33] and thus the uptake of electrons in these species takes place on the macrocycle, this latter unit undergoing all reductions. It is therefore reasonably postulated that the conjugated TTDPz macrocycle is also the site for all of the observed reduction processes of these compounds.

The first two reductions of TTDPz derivatives are best defined in DMF or pyridine, and the majority of our discussion on the electrochemical data is therefore limited

(26) Clack, D. W.; Hush, N. S.; Woolsey, I. S. *Inorg. Chim. Acta* **1976**, *19*, 129.
(27) Lever, A. B. P.; Minor, P. C. *Inorg. Chem.* **1981**, *20*, 4015.
(28) Giraudeau, A.; Fau, F. F.; Bard A. J. *J. Am. Chem. Soc.* **1980**, *102*, 5137.
(29) Guilard, R.; Zrineh, A.; Tabard, A.; Endo, A.; Han, B. C.; Lecomte, C.; Souhassou, M.; Habbou, A.; Ferhat, M.; Kadish, K. M. *Inorg. Chem*. **1990**, *29*, 4476.
(30) Kadish, K. M.; Cornillon, J.-L.; Coutsolesos, A.; Guilard, R. *Inorg. Chem*. **1987**, *26*, 4167.
(31) Cornillon, J.-L.; Anderson, J. E.; Kadish, K. M. *Inorg. Chem*. **1986**, *25*, 2611.
(32) (a) L'Her, M.; Pondaven, A. In *The Porphyrin Handbook*; Kadish, K. M., Smith, K. M., Guilard, R., Ed.; Academic Press: Amsterdam, 2003; Vol. 16, Chapter 104, p 117. (b) Lever, A. B. P.; Milaeva, E. R.; Speier, G. In *Pthalocyanines: Properties and Applications*; Lever, A. B. P., Leznoff, C. C., Eds.; VCH Publ. Inc.: New York, 1993; Vol. 3, p 1.
(33) Kadish, K. M.; van Caemelbecke, E.; Royal, G. In *The Porphyrin Handbook*; Kadish, K. M., Smith, K. M., Guilard, R., Eds.; Academic Press: Amsterdam, 2000; Vol. 8, Chapter 55, p 1.

Table 6. Half-Wave Potentials (V vs SCE) of [PcMX], [TTDPzMX], and Related Porphyrins in Different Solvents

				$E_{1/2}$, redn				$\Delta E_{1/2}$			
macrocycle	M	X	solvent	first	second	third	fourth	Δ_{1-2}	Δ_{2-3}	Δ_{3-4}	ref
Pc	Al	Cl^-	py	−0.55	−0.90	−1.78[a]		0.35	0.88		tw
	Ga	Cl^-		−0.53[a,b]	−0.84	−1.73[a]		0.41	0.89		tw
	In	Cl^-		−0.67	−0.94	−1.83[a]		0.27	0.89		tw
	Al	Cl^-	DMF	−0.55	−1.00	−1.94		0.45	0.94		tw
				−0.53	−0.98[c]	−1.98		0.45	1.00		26
				−0.66							27
			DMA	−0.50	∼−1.1	∼−1.9					28
	Ga	Cl^-		−0.49	−0.88[d]	−1.85		0.39	0.97		tw
	In	Cl^-		−0.63	−1.15[a]	−1.84[a]		0.52	0.69		tw
TTDPz	Al	Cl^-	py	−0.07	−0.54	see Figure 7		0.47			tw
		OH^-		−0.29	−0.66	−1.36	−1.75	0.37	0.70	0.39	tw
	Ga	Cl^-		−0.13	see Figure 8						tw
		OH^-		−0.13	see Figure 8						tw
	In	OAc^-		−0.26							tw
	Al	Cl^-	DMF	−0.10	−0.54[e]	−1.34[f]	−1.78	0.49	0.80	0.44	tw
		Cl^-[g]		−0.19	−0.56	−1.31	−1.75	0.37	0.75	0.44	tw
		OH^-		−0.12	−0.56	−1.36[h]	−1.80	0.44	0.80	0.44	tw
	Ga	OH^-		−0.07	−0.47	−1.31[i]	−1.82	0.40	0.84	0.51	tw
OEP	Al	Cl^-	CH_2Cl_2	−1.38							29
	Ga	Cl^-	py	−1.15	−1.70			0.55			30
			CH_2Cl_2	−1.38	−1.81			0.43			30
	In	OAc^-	py	−1.30							31
TPP	Al	Cl^-	CH_2Cl_2	−1.10	−1.45			0.35			30
	Ga	Cl^-	py	−0.86	−1.40			0.54			30
			CH_2Cl_2	−1.12	−1.52			0.40			30
	In	OAc^-	py	−1.64							31

[a] E_{pc} at a scan rate of 0.1 V/s. [b] A peak at $E_{pc} = -0.40$ V can also be seen. [c] A reduction at −1.42 V was reported. [d] A reduction at −1.50 V can also be seen. [e] A peak at $E_{pc} = -0.48$ V can also be seen. [f] A peak at $E_{pc} = -1.16$ V can also be seen. [g] Excess Cl^- added as the TBACl form. [h] A reversible reduction can also be seen at −0.79 V. [i] A reversible reduction can also be seen at −0.79 V. tw = this work.

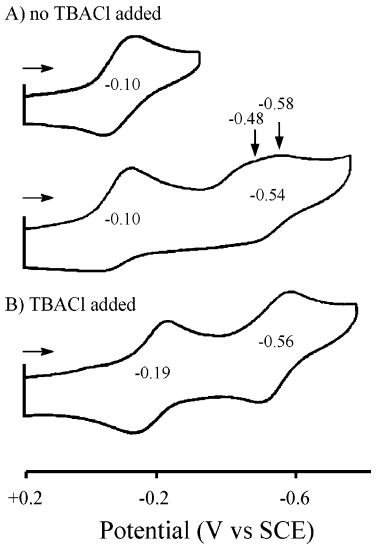

Figure 5. Cyclic voltammogram of [TTDPzAlCl] in DMF, 0.1 M TBAP, (a) before and (b) after addition of excess TBACl to solution. Scan rate = 100 mV/s.

to these two one-electron additions since a detailed examination of equilibria and electrochemical mechanisms involving the more highly charged anionic species is beyond the scope of the present manuscript and perhaps more appropriate for a specialized journal.

The demonstration of one such equilibria involving [TTDPzAlCl] is shown by the cyclic voltammograms in Figure 5, which illustrates the first two reductions of the compound in DMF, 0.1 M TBAP, before and after the addition of TBACl to solution. The initial one-electron reduction is located at $E_{1/2} = -0.10$ V in DMF, 0.1 M TBAP, and is reversible when the negative potential sweep is reversed at −0.40 V (Figure 5A). However, this process becomes irreversible and involves a coupled chemical reaction on the reoxidation step when the return scan is initiated at −0.80 V (Figure 5A), a point negative of the second reduction which is split into two closely spaced processes at $E_p = -0.48$ and −0.58 V for a scan rate of 0.10 V/s.

The type of current−voltage curves for first reduction in Figure 5 are what would be expected for an equilibrium involving [TTDPzAlCl] and solvated $[TTDPzAl(DMF)_x]^+$, the latter of which should be easier to reduce by virtue of the overall positive charge on the complex.

This equilibrium is shown in eq 1 and can be shifted to the left by the addition of excess Cl^- to solution. This is illustrated by the cyclic voltammogram in Figure 5B, where $E_{1/2}$ for the first reduction shifts from −0.10 to −0.19 V. The reduction at $E_{1/2} = -0.10$ V is assigned to the DMF solvated form of the Al^{III} complex while the process at $E_{1/2} = -0.19$ V is assigned as a reduction of the compound which still maintains the bound Cl^- anion.

$$[TTDPzAlCl] + x\text{DMF} = [TTDPzAl(DMF)_x]^+ + Cl^- \quad (1)$$

Equilibria involving different DMF-solvated forms of electroreduced [TTDPzAlCl] are also seen by the differential pulse voltammogram (DPV) shown in the top of Figure S2 (see Supporting Information). The DPV experiment is carried out at a slower scan rate (5−10 mV/s) than cyclic voltammetry (100 mV/s or greater), and under these experimental conditions the first one-electron addition proceeds exclusively via the more easily reduced form of the compound not having

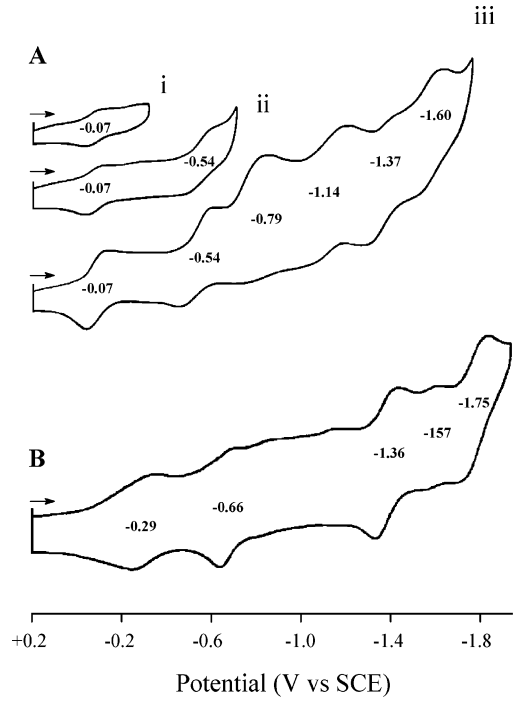

Figure 6. Cyclic voltammograms of (A) [TTDPzAlCl] in pyridine, 0.1 M TBAP (i and ii, first scan; iii, second scan) and (B) [TTDPzAlOH] (second scan only) in pyridine, 0.1 M TBAP. Scan rate = 100 mV/s.

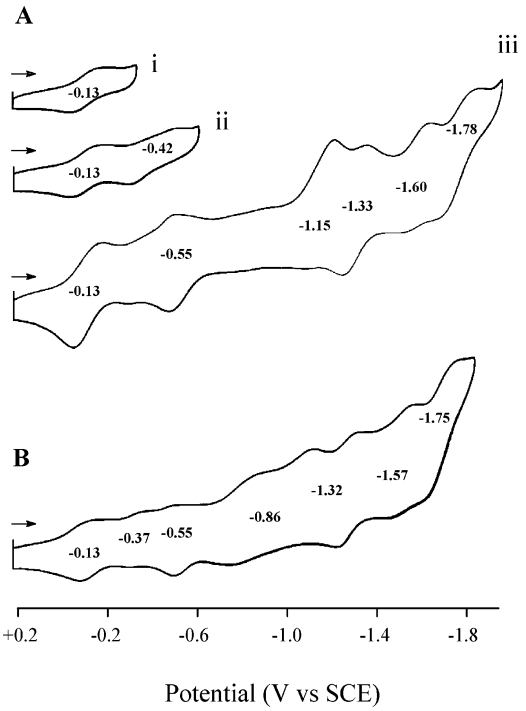

Figure 7. Cyclic voltammograms of (A) [TTDPzGaCl] in pyridine, 0.1 M TBAP (i and ii, first scan; iii, second scan; TLCV, scan rate 20 mV/s) and (B) [TTDPzGaOH] (second scan only) in pyridine. Scan rate = 100 mV/s.

the Cl^- axial ligand. The lack of an observable equilibrium in the first reduction contrasts with what is seen on the next three one-electron additions where each redox process is characterized by two reduction peaks whose relative current heights vary with the concentration of the electroactive species (see later section). At the highest investigated [TTDPzAlCl] concentration (1.21 mM), the second reduction is characterized by peaks at $E_p = -0.43$ and -0.71 V, while the third and fourth reductions are located at peak potentials of -1.05 and -1.25 V and -1.54 and -1.72 V, respectively. Similar potentials and similar equilibria are also seen for [TTDPzAlOH] in DMF, and this is illustrated by the differential pulse voltammogram in the lower half of Figure S2.

An equilibrium of the type shown in eq 1 also occurs for [TTDPzAlCl] and [TTDPzAlOH] in pyridine, where the first or first and second reductions are fairly well-defined and those at more negative potentials are characterized by multiple equilibria as shown by the cyclic voltammograms in Figure 6A. The first reversible reduction of [TTDPzAlCl] occurs at $E_{1/2} = -0.07$ V in pyridine and involves the solvated form of the compound without the chloride axial ligand while the first reduction of [TTDPzAlOH] is located $E_{1/2} = -0.29$ V under the same solution conditions and involves the complex with the hydroxide counterion still associated. In both cases, the product of the one-electron reduction is the π-anion radical where the electron is localized on the macrocycle. Although the first two reductions of [TTDPzAlOH] in pyridine give less well-defined current−voltage curves than [TTDPzAlCl], the overall voltammogram for the hydroxide derivative is better defined with respect to showing the expected[4b,5b,26] four reductions on the second scan. This is illustrated in Figure 6B, where the $E_{1/2}$ values are -0.29, -0.66, -1.36, and -1.75 V for the four major redox processes.

Results similar to those of [TTDPzAlX] ($X = Cl^-$, OH^-) were obtained for the Ga^{III} complexes in pyridine. The first reduction of [TTDPzGaCl] is located at $E_{1/2} = -0.13$ V vs SCE by cyclic voltammetry and shows a good reversibility (Figure 7A). However, a complex situation is again seen for the processes at more negative potentials. This behavior is due to an involvement of the electroreduced species in one or more chemical reactions, some or all of which involve pyridine. A similar behavior has been reported for Ga^{III} porphyrins in coordinating solvents.[30]

The Ga^{III} hydroxide species, [TTDPzGaOH], also exhibits a reversible first reduction at $E_{1/2} = -0.13$ V plus a number of other processes similar to what is observed in the case of the Ga^{III} chloride derivative. The fact that no difference is observed in $E_{1/2}$ for the first reduction of [TTDPzGa^{III}Cl] or [TTDPzGa^{III}OH] can be accounted for by a dissociation of the Cl^- and OH^- ligands in pyridine solutions, thus giving the same electroactive species, which is assigned as $[TTDPzGa(py)_x]^+$, where $x = 1$ or 2.

Ill-defined reductions are seen for the In^{III} complex, [TTDPzIn(OAc)], although the first reduction at $E_{1/2} = -0.26$ V seems to be clear. Several additional ill-defined peaks are present on the cathodic or anodic potential scans, and these are due to different coordinated forms of the electroreduced species which exist in pyridine.

As can be seen in Table 6, the first one-electron reductions of the [TTDPzMX] complexes are all extremely facile. The process at $E_{1/2} = -0.07$ V for [TTDPzAlCl] and -0.13 V [TTDPzGaCl] in pyridine gives in both cases the π-anion

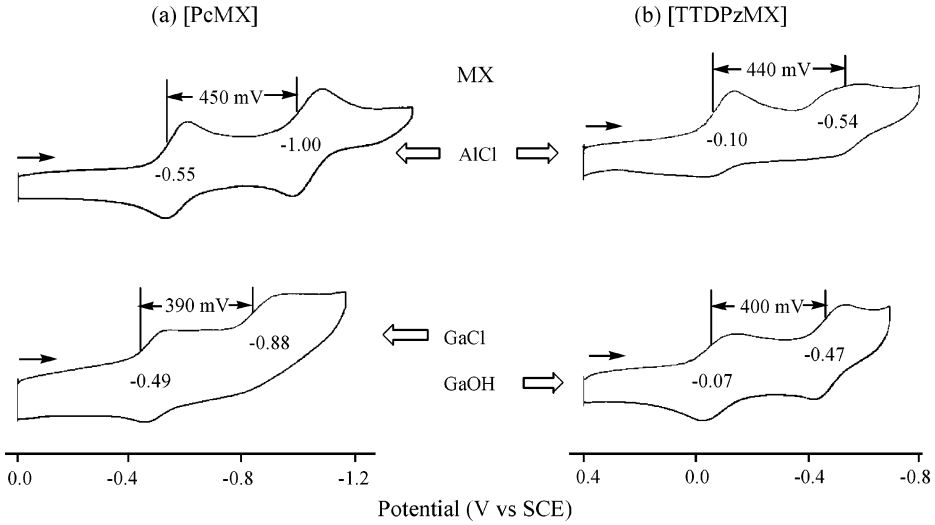

Figure 8. Cyclic voltammograms of (a) [PcMX] and [TTDPzMX], where M = Al^{III} or Ga^{III} and X = Cl^- or OH^- in DMF, 0.1 M TBAP.

radical [TTDPzM$(py)_x$], where $x = 1$ or 2. The second reduction of [TTDPzMX] gives the dianion and is also quite facile. Worthy of notice, the measured $E_{1/2} = -0.54$ V for the second reduction of [TTDPzAlCl] in pyridine or DMF is virtually identical with the half-wave potential for the first reduction of [PcAlCl] in the same solvent/supporting electrolyte mixture (−0.55 V vs SCE). Moreover, as can be seen from the data in Table 6, not only do the first two reductions of [TTDPzAlCl] occur at potentials considerably less negative than the corresponding redox reactions of [PcAlCl] but the measured half-wave potentials are shifted even further in a positive direction from $E_{1/2}$ values for reduction of the related main group metalloporphyrins (OEP and TPP) containing an Al^{III} central ion. These data thus provide clear evidence that a replacement of the benzene rings in the phthalocyanine macrocycle by strongly electron-deficient thiadiazole rings highly facilitates the electron uptake and associated negative charge redistribution within the macrocycle.

Additional Comparisons between [TTDPzMX] and [PcMCl]. The reduction of [PcMCl] (M = Al^{III}, Ga^{III}, or In^{III}) was examined in DMF and pyridine for comparison with the TTDPz complexes under the same experimental conditions. The half-wave potentials in both solvents are listed in Table 6, which also includes data from the literature for the same compounds under similar solution conditions.[26,27]

A comparison of how the change in macrocycle from Pc to TTDPz affects redox potentials of the first two reductions is given in Figure 8, which shows cyclic voltammograms for the Al^{III} and Ga^{III} complexes of each macrocycle in DMF. [PcM], where M = Mg^{II}, Zn^{II}, or Cu^{II}, undergoes three or four major one-electron reductions within the negative potential limit of the solvent. The first two of these are located at $E_{1/2} = -0.89$ and −1.33 V vs SCE for [PcZn] and at −0.66 and −1.06 V for [PcH_2].[26] The first two reductions of the main group Pc complexes occur at more positive potentials as seen for [PcAlCl] (−0.55 and −1.00 V) and [PcGaCl] (−0.49, −0.88 V), and this is expected on the basis of the electronegativity of the central metal ion.

Changing from a transition metal phthalocyanine to a main group phthalocyanine leads to positive potential shift in all reduction potentials, and for a comparison of [PcZn] to [PcAlCl] in DMF, the $\Delta E_{1/2}$ amounts to 340 mV for the first reduction and 330 mV for the second.[26] A much larger shift in $E_{1/2}$ is seen upon changing the macrocycle from Pc to TTDPz, and here the $\Delta E_{1/2}$ between the first two reductions of the Al−Cl species in DMF amounts to 450−460 mV, with the easiest reductions being observed for the TTDPz derivatives (see Figure 8).

The same trend is observed when comparing cyclic voltammograms of [PcGaCl] and [TTDPzGaOH] (Figure 8). Here the positive potential shift in $E_{1/2}$ for the ring-centered reductions of TTDPz complexes ranges from 410 to 420 mV, again with the TTDPz derivative being easier to reduce than the Pc complex. For example the π-anion radical of [TTDPzGaOH] is generated at $E_{1/2} = -0.07$ V, and the same reaction of [PcAlCl] occurs at $E_{1/2} = -0.55$ V. At the same time, the value of $\Delta E_{1/2}$ between potentials for formation of the π-anion radical and dianion remains constant for a given metal ion (Al^{III} or Ga^{III}) in the Pc and TTDPz series (390−450 mV as indicated in the figure), and this is consistent with the same degree of electron delocalization in the π-anion radical and dianion.

As indicated above, the equilibria involving different solvated forms of electroreduced [TTDPzAlCl] could be shifted by changes in the concentration of the electroactive species, and this is shown by the differential pulse voltammograms in Figure S3 (see Supporting Information) which also includes data on [PcAlCl]. As seen in this figure, the first two reductions of [PcAlCl] (at −0.52 and −0.97 V) are separated by 450 mV, which is virtually the same potential separation between the first two reductions of [TTDPzAlCl] (−0.07 and −0.51 V). The first and second reductions of the most dilute [TTDPzAlCl] solution are also easier than the first two reductions of [PcAlCl] by 450−460 mV, and this suggests that the singly and doubly reduced Al^{III} complexes both possess the same degree of solvation, independent of the type of macrocycle, Pc or TTDPz. The peak current for the second reduction of [TTDPzAlCl] at

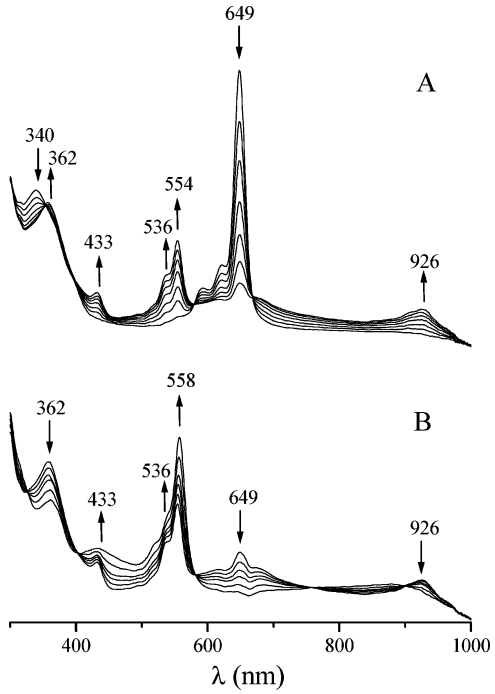

Figure 9. UV−vis spectral changes in pyridine containing 0.2 M TBAP during controlled-potentials electrolysis of [TTDPzAlCl] at (A) −0.34 V (first reduction, first scan) and (B) −0.70 V (second reduction, first scan).

−0.51 V also increases in magnitude with dilution as the current for the peak at −0.71 V decreases (Figure S3), and this result is consistent with the first, easier, reduction involving generation of a dianion with two axially bound DMF molecules and the second harder reduction giving a dianion with just a single axially coordinated DMF. The proposed mechanism for reduction of [TTDPzAlCl] is then as shown in Scheme S1 (see Supporting Information) and is the subject of further investigations also involving the other metalated complexes in different solvents.

Spectroelectrochemical Measurements. Time-resolved thin-layer spectra were obtained during the electroreduction of [TTDPzMX] in pyridine. The spectral changes which occur during the first two one-electron reductions of the Al^{III} complex, [TTDPzAlCl], are shown in Figure 9. Full regeneration of the initial spectrum upon stepwise reoxidation of the doubly reduced complex to its neutral form confirms the full reversibility of the first two redox processes.

Figure 9A shows the spectral changes which occur during first reduction of [TTDPzAlCl] at a fixed applied potential of −0.34 V vs SCE to give [TTDPzAl] as a final product. The practically complete disappearance of the intense Q band at 649 nm is accompanied by a shift of the B band from 340 to 362 nm and the appearance of new bands at 433, 536 (sh), 554, and 926 nm.

Quite similar spectral changes are seen during the first one-electron reduction of the Ga^{III} and In^{III} analogues, [TTDPzGaCl] and [TTDPzIn(OAc)]. The combined disappearance of the intense Q band and the appearance of bands of lower intensity in the regions of 500−600 and 800−1000 nm are strongly indicative for formation of π-anion radicals, as exemplified by the chemical one-electron reduction of the Al^{III} phthalocyanine species [PcAlCl] to its monoanionic form, [PcAl]. The Pc π-anion radical shows low-intensity absorptions at 575, 595, and 975 nm and lacks the intense Q band at 662 nm observed for neutral [PcAlCl].[34] According to theoretical work on metal phthalocyanines,[35] the bands at ca. 920 nm seen in the spectra of singly reduced [TTDPzAlCl] and [TTDPzGaCl] can be assigned as a shifted Q band. The bands at 530−560 nm for the π-anion radial are assigned as due to $\pi^* \rightarrow \pi^*$ transitions involving an orbital containing the unpaired electron and the band near 420−450 nm is assigned to the second $\pi \rightarrow \pi^*$ transition. A band in the near-IR region (at 800−900 nm) was also observed for π-anion radicals formed by the one-electron reduction of Ga^{III} porphyrins.[30]

Electrogeneration of the dianionic Al^{III}, Ga^{III}, and In^{III} species $[TTDPzM]^-$ at −0.7 to −0.8 V gives spectral changes which consist mainly of a strong intensification with minor shifts of the absorption bands assigned to the $\pi^* \rightarrow \pi^*$ transitions at 530−560 nm, accompanied by some shifts and changes of the lower intensity first and second $\pi \rightarrow \pi^*$ transitions. This is illustrated in Figure 9B which shows the spectral changes which occur during the second reduction of [TTDPzAlCl] to give $[TTDPzAl]^-$. It is known from the literature[35] that the characteristic feature of the second reduction and formation of the π-dianion for metal phthalocyanine complexes with redox-inactive central metals is a hypsochromic shift of the $\pi^* \rightarrow \pi^*$ transition band which retains its intensity.

UV−visible spectra were also recorded during reduction of the Al^{III} and Ga^{III} complexes at more negative fixed potential values of −1.3 to −1.5 V. These reductions result in only minor changes in the position of the $\pi^* \rightarrow \pi^*$ transition band at 540−560 nm in the first step, but more dramatic spectral modifications take place in the second. The spectral changes consist in a complete disappearance of the band at 540−560 nm and the appearance of one new band at 480−490 nm and another close to 600 nm. Such spectral variations must involve changes in the energy and population of the π and π^* orbitals of the macrocyclic ligand.

Conclusion

As shown in the present contribution, direct template condensation of 3,4-dicyano-1,2,5-thiadiazole with appropriate metal salts, which did not work for the synthesis of previously described tetrakis(thiadiazole)porphyrazines containing bivalent first-raw transition metal ions,[2b] was found to be successful as a procedure for the preparation of main group tervalent metal ion derivatives having the formula [TTDPzMX] (M = Al^{III}, Ga^{III}, In^{III}; X = Cl^-, Br^-, OAc^-) and the OH^- species therefrom in the case of Al^{III} and Ga^{III}, i.e., [TTDPzMOH]. This is promising in view of an extension of synthetic work directed to the preparation of new selected metal derivatives of the TTDPz macrocycle. A single-crystal X-ray study of [TTDPzMCl] (M = Al^{III}, Ga^{III}) indicates that the presence of heteroatoms (S, N) in the annulated thiadia-

(34) Clack, D. W.; Yandle, J. R. *Inorg. Chem.* **1972**, *11*, 1738.
(35) Mack, J.; Stillman, M. J. In *The Porphyrin Handbook*; Kadish, K. M., Smith, K. M., Guilard, R., Eds.; Academic Press: Amsterdam, 2000; Vol. 8, Chapter 55, p 1.

zole rings of the porphyrazine macrocycle plays an important role in determining the interunit contacts in the crystalline materials for the two isostructural species. This role was expected,[2a] and further confirmation was also recently achieved by an X-ray study of the free-base [$TTDPzH_2$] and a series of its bivalent metal derivatives.[8] The IR and UV−vis spectra in this paper provide information for characterization of the monometallic species [TTDPzMX], both in the solid state and in solution. The electrochemical measurements show a reversibile formation of the π-anion radical and dianion, but complicated processes are seen at more negative potentials. The facile uptake of electrons is strictly connected with σ- and π-electron-withdrawing effects of the macrocycle due to the externally annulated thiadiazole rings. This is particularly evident when the measured potentials are compared with potentials in the literature for reduction of the phthalocyanine and porphyrin derivatives with the same main group metal ions. Furthermore, the observed electrochemical behavior closely approaches what was recently reported for a new class of "pyrazinoporphyrazines". This is due to the presence in these latter species of strongly electron-attracting dipyridinopyrazino fragments directly annulated to the central porphyrazine core.[5]

Experimental Section

Solvents and Chemicals. Solvents (acetone, benzene, CH_2Cl_2, THF, pyridine, hexane, dimethyl sulfoxide (DMSO), acetic acid, and methanol) and reagents ($AlCl_3$, $AlBr_3$, $GaCl_3$, $In(OH)(AcO)_2$) were pure chemicals (Carlo Erba, Aldrich, Merck, Reakhim). Quinoline (Quin) and 1-chloronaphthalene (ClNP) were freshly distilled over CaH_2 before use. Benzene was made anhydrous by distillation over potassium. 3,4-Dicyano-1,2,5-thiadiazole (DCTD) was obtained from diaminomaleodinitrile and thionyl chloride according to the procedure reported elsewhere.[2]

(Tetrakis(1,2,5-thiadiazole)porphyrazinato)aluminum(III) Chloride Solvate, [TTDPzAlCl](H_2O)$_4$(quin). This complex was prepared by direct synthesis starting from DCTD and $AlCl_3$, following a previously described procedure reported for the synthesis of [PcAlCl].[10] A mixture of $AlCl_3$ (530 mg, 3.97 mmols) and DCTD (2.16 g, 15.88 mmol) in freshly distilled quinoline (6 mL) was kept refluxing for 3 h in an inert atmosphere. The reaction mixture, initially straw-colored, became reddish and then dark green, and a dark blue-green precipitate was formed. After cooling, the solid was separated by rapid centrifugation, washed with small portions of anhydrous benzene and acetone, and brought to constant weight under vacuum (10^{-2} mmHg; 1.35 g, yield 56%). Anal. Calcd for [TTDPzAlCl](H_2O)$_4$(quin), $C_{25}H_{15}AlClN_{17}O_4S_4$ (MW: 808.18): C, 37.15; H, 1.87; N, 29.47; S, 15.87. Found: C, 37.86; H, 1.62; N, 26.71; S, 15.66. IR (cm^{-1}): 1640 w, 1597 w, 1530 m s, 1300 vw, 1280 vs, 1115 vw, 1090 s, 1060 w, 980 vw, 887 w m, 832 w, 810 w m, 790 vw, 772 w, 744 m s, 695 vs, 615 vw, 518 s, 480 w, 405 w, 373 w, 347 m s, 315 w, 298 w, 283 w. After elimination of H_2O and quinoline, the complex is stable in a dried atmosphere up to temperatures >300−350 °C. In air it slowly (1 day) changes into the corresponding hydroxide. The solid is slightly soluble in pyridine, DMSO, and ClNP and almost insoluble in quinoline. TGA shows three distinct weight losses corresponding to ca. two clathrated water molecules (50−100 °C), two additional water molecules probably interacting with the chlorine atom or bridging two complex molecules (100−200 °C), and one molecule of quinoline (ca. 300 °C).

(Tetrakis(1,2,5-thiadiazole)porphyrazinato)aluminum(III) Hydroxide Solvate [TTDPzAlOH](H_2O)$_5$(quin)$_{0.5}$. [TTDPzAlCl]-(H_2O)$_4$(quin) (200 mg, 0.33 mmol) was suspended in H_2O (10 mL), and the mixture was kept refluxing with stirring for 3 h. After cooling, a blue solid was separated by centrifugation and brought to constant weight under vacuum (10^{-2} mmHg). Yield: 170 mg (92%). Anal. Calcd for [TTDPzAlOH](H_2O)$_5$(quin)$_{0.5}$, $C_{20.5}H_{14.5}AlN_{16.5}O_6S_4$ (MW: 743.18): C, 33.13; H, 1.97; N, 31.10; S, 17.25. Found: C, 32.73; H, 1.34; N, 30.85; S, 17.48. IR (cm^{-1}): 1630 m w, 1535 m s, 1305 vw, 1280 vs, 1120 vw, 1090 s, 1060 m w, 887 w m, 830 w, 790 vw, 765 w, 740 s, 695 s, 630 w m, 515 s, 455 vw, 400 vw, 360 vw, 330 vw, 315 vw, 298 vw, 280 vw. The solid is slightly soluble in DMSO, quinoline, and pyridine and insoluble in CH_2Cl_2. TGA shows weight losses corresponding to clathrated water molecules (50−100 °C), additional water molecules probably hydrogen bonded and more strongly retained, and a residual amount of quinoline (>100 °C).

(Tetrakis(1,2,5-thiadiazole)porphyrazinato)aluminum(III) Bromide Trihydrate, [TTDPzAlBr](H_2O)$_3$. A mixture of $AlBr_3$ (660 mg, 2.47 mmols) and DCTD (1.34 g, 9.84 mmol) in freshly distilled quinoline (10 mL) was kept refluxing for 3 h with stirring in an inert atmosphere. After cooling, the blue solid was separated by filtration under N_2, washed with anhydrous benzene and acetone until colorless washings, and brought to constant weight under vacuum (10^{-2} mmHg). Yield: 630 mg (39%). Anal. Calcd for [TTDPzAlBr](H_2O), $C_{16}H_6AlBrN_{16}O_3S_4$ (MW: 705.45): C, 27.24; H, 0.86; N, 31.77; S, 18.18. Found: C, 27.95; H, 1.03; N, 31.24; S, 17.50. IR (cm^{-1}): 1635 vw, 1590 vw, 1535 w, 1275 s, 1085 s, 885 s, 830 w, 812 m s, 790 m s, 768 s, 742 vs, 695 vs, 612 m, 515 vs, 475 m, 405 w m, 380 w, 360 w, 330 s, 300 w m, 255 w m. The complex is stable in a dry atmosphere. In air it slowly (2 days) changes into its corresponding hydroxide, which is also formed in water solution similarly to what is described above for the AlCl species.

(Tetrakis(1,2,5-thiadiazole)porphyrazinato)gallium(III) Chloride Solvate, [TTDPzGaCl](H_2O)$_2$(quin). A mixture of $GaCl_3$ (110 mg, 0.62 mmols), handled in a drybox, and DCTD (342 mg, 2.5 mmols) in freshly distilled quinoline (3 mL) was heated at 180 °C for 3 h with stirring in an inert atmosphere. After cooling, the blue microcrystalline solid was separated by a rapid centrifugation, washed with anhydrous benzene and acetone, and brought to constant weight under vacuum (10^{-2} mmHg). Yield: 140 mg (35%). Anal. Calcd for [TTDPzGaCl](H_2O)$_2$(quin), $C_{25}H_{11}ClGaN_{17}O_2S_4$ (MW: 814.89): C, 36.85; H, 1.36; N, 29.22; S, 15.74. Found: C, 37.64; H, 1.08; N, 29.90; S, 15.29. IR (cm^{-1}): 1690 w, 1645 w, 1597 w, 1535 m, 1502 w, 1275 s, 1130 vw, 1120 vw, 1090 s, 1062 m, 945 vw, 880 s, 815 vs, 790 s, 735 s, 735 vs, 690 vs, 615 m, 560 w, 518 vs, 480 s, 455 w, 382 s, 300 m w, 260 w. The complex is stable in a dried atmosphere and can be heated to a temperature higher than 400 °C. In air it slowly changes into its corresponding hydroxide (days).

(Tetrakis(1,2,5-thiadiazole)porphyrazinato)gallium(III) Hydroxide Dihydrate, [TTDPzGaOH](H_2O)$_2$. [TTDPzGaCl]-(H_2O)$_2$(quin) (65 mg, 79.76 mmols) was suspended in H_2O (4 mL), and the mixture was kept refluxing for 3 h. After cooling, the solid was separated by centrifugation, washed with water, and dried under vacuum (10^{-2} mmHg). Yield: 38 mg (78.3%). Anal. Calcd for [TTDPzGaOH](H_2O)$_2$, $C_{16}H_5GaN_{16}O_3S_4$ (MW: 667.28): C, 28.80; H, 0.76; N, 33.59; S, 19.22. Found: C, 29.16; H, 0.67; N, 33.73; S, 18.94. IR (cm^{-1}): 1700 vw, 1645 w m, 1540 m, 1508 w m, 1280 s, 1067 m, 885 vs, 875 w, 837 s m, 820 s m, 795 m, 772 s, 740 vs, 695 vs, 630 vw, 620 w, 565 w, 520 vs, 483 m, 460 m w, 362 vw, 300 m, 262 s m, 250 m.

(Tetrakis(1,2,5-thiadiazole)porphyrazinato)indium(III) Acetate, [TTDPzIn(OAc)]. [$TTDPzH_2$] (100 mg, 1.54 mmols) was added to a boiling solution of basic indium acetate $In(OH)(AcO)_2$ (200 mg, 3.0 mmols) in acetic acid (30 mL). The mixture was refluxed with stirring for 2 h until its green color turned a bluish shade. After cooling, the mixture was poured into water and filtered. To remove excess $In(OH)(AcO)_2$, the product was washed with a mixture of equal parts of acetic acid and water and then with distilled water until neutrality. The product was washed in a Soxhlet with methanol and dried in a vacuum (10^{-2} mmHg). Yield: 78 mg (55%). Anal. Calcd for $[TTDPzIn(OAc)](H_2O)_2$, $C_{18}H_3InN_{16}O_2S_4$ (MW: 718.39): C, 30.09; H, 0.42; N 31.20; S, 17.85. Found: C, 30.17; H, 1.18; N, 31.51; S, 18.73.

Electrochemical and Spectroelectrochemical Measurements. Cyclic voltammetry (CV) and differential pulse voltammetry (DPV) measurements were performed at 298 K on an EG&G model 173 potentiostat coupled with an EG&G model 175 universal programmer or an EG&G Model 263 potentiostat. The solvents were pyridine (Aldrich, anhydrous, 99.8%) or dimethylformamide (DMF) (Aldrich, anhydrous, 99.8%) containing 0.1 M tetrabutylammonium perchlorate (TBAP) as supporting electrolyte. High-purity N_2 from Trigas was used to deoxygenate the solution before each electrochemical experiment. TBAP was purchased from Sigma Chemical or Fluka Chemika Co., recrystallized from ethyl alcohol, and dried under vacuum at 40 °C for at least 1 week prior to use. A three electrode system was used and consisted of a glassy carbon working electrode, a platinum wire counter electrode, and a saturated calomel reference electrode (SCE). The reference electrode was separated from the bulk of the solution by a fritted-glass bridge filled with the solvent/supporting electrolyte mixture. Thin-layer spectroelectrochemistry measurements were carried out with an optically transparent platinum thin-layer working electrode using a Hewlett-Packard model 8453 diode array spectrophotometer coupled with an EG&G model 173 universal programmer. These measurements were carried out in solutions containing 0.2 M TBAP as supporting electrolyte.

Kinetic Measurements. After a sample of the species [TTDPzMX] (MX = AlCl, GaCl, In(OAc)) was dissolved in 16.9 M H_2SO_4 (91%) the solution was promptly filtered through a glass filter and placed in a quarz cuvette in the Hitachi U-2000 spectrophotometer equipped with a thermostated cuvette holder. The spectral curves were registered at 90 s time intervals, or the kinetic curves were recorded at a fixed wavelength corresponding to the maximum of the Q-band of the complex. Since the kinetic curves follow a first-order law, the observed rate constants were calculated using

$$k_{obs} = (1/\tau) \ln[(A - A_\infty)/(A_0 - A_\infty)] \quad (2)$$

where A_0, A_∞, and A are the absorbances of the solution at the analytical wavelengths at the beginning, at the end, and in the course of the reaction, respectively. In the case of very slow reactions when A_∞ was not achieved, the k_{obs} values were calculated using the Huggenheim approach.

Crystal Structure Determination. X-ray diffraction data were collected at 173 K with graphite-monochromated Mo Kα (λ = 0.710 73 Å) radiation on a Rigaku Mercury CCD diffractometer. All structures were solved by a direct method using the SHELXS-97 program[36] and refined by successive differential Fourier syntheses and a full-matrix least-squares procedure using the SHELXL-97 program.[37] Isotropic thermal factors were applied to some atoms except Al and Cl atoms for [TTDPzAlCl]. The highest residual electron peak was 3.41 $e^-/Å^3$ at a distance of 0.70 Å from the nitrogen atom in [TTDPzAlCl], owing to the poor crystallinity.

Other Physical Measurements. IR spectra were taken with a Perkin-Elmer 783 spectrophotometer in the range of 4000−200 cm^{-1} by using Nujol mulls between CsI plates. UV−vis spectra were taken with a Varian Cary 5E spectrometer. Thermogravimetric analyses (TGA) were performed on a Stanton Redcroft model STA-781 analyzer under an N_2 atmosphere (0.5 L/min). Elemental analyses for C, H, N, and S were provided by the Servizio di Microanalisi at the Dipartimento di Chimica, Università "La Sapienza" (Rome), on a EA 1110 CHNS-O instrument.

Acknowledgment. Financial support by the University of Rome "La Sapienza" and the MIUR (Cofin 2003038084) and the Robert A. Welch Foundation (K.M.K, Grant E-680) is gratefully acknowledged. Support by the bilateral exchange program active between the University of "La Sapienza" (Rome, C.E.) and the Ivanovo State University of Chemical Technology (Ivanovo, P.A.S.) is also acknowledged. M.P.D. is grateful to the Department of Chemistry, University of Houston, for kind hospitality. S.S.I. thanks the Russian Ministry of Education and Science for financial support (Grant A03-2.11-349). Thanks are expressed to Dr. Z. Ou (Houston) for help with some electrochemical experiments and Dr. Paola Galli (Rome) for useful discussions.

Supporting Information Available: X-ray crystallographic files in CIF format for the structure determination of the complexes [TTDPzAlCl] and [TTDPzGaCl], Figures S1 (IR spectra) and S2 and S3 (electrochemistry) and Scheme S1 (scheme for electroreduction mechanism). This material is available free of charge via Internet at htpp://pubs.acs.org.

IC050866B

(36) Sheldrick, G. M. *SHELXS-97: Program for crystal structure solution*; University of Göttingen: Göttingen, Germany, 1997.
(37) Sheldrick, G. M. *SHELXL-97: Program for crystal structure refinement*; University of Göttingen: Göttingen, Germany, 1997.